Modern Physics Letters A

IMPLEMENTATION OF THE ATLAS-SUSY-2018-04 ANALYSIS IN THE MADANALYSIS 5 FRAMEWORK

Jongwon Lim
Department of Physics, Hanyang University, Seoul 04763, Republic of Korea

Chih-Ting Lu
School of Physics, KIAS, Seoul 02455, Republic of Korea

Jae-hyeon Park
School of Physics, KIAS, Seoul 02455, Republic of Korea

Jiwon Park
Department of Physics, Hanyang University, Seoul 04763, Republic of Korea

Received (Day Month Year)
Revised (Day Month Year)

We present the MADANALYSIS 5 implementation and validation of the ATLAS-SUSY-2018-04 search. This ATLAS analysis targets the search for direct stau production in events with two hadronic tau leptons and probes 139 fb^{-1} of LHC proton-proton collisions at a center-of-mass energy of 13 TeV. The validation of our reimplementation relies on a comparison of our cutflow predictions with the auxiliary table of official ATLAS results in the context of two supersymmetry-inspired simplified benchmark models in which the Standard Model is extended by a neutralino and a stau decaying into a tau lepton and a neutralino.

Keywords: supersymmetry; stau; hadronic tau lepton.

1. Introduction

In this note, we describe the validation of the implementation, in MADANALYSIS 5 framework,[1–4] of the ATLAS-SUSY-2018-04 search[5] for direct stau production in two hadronic $\tau + E_T^{miss}$ events. This process is illustrated by the representative Feynman diagram of Fig. 1. This analysis focuses on LHC proton-proton collisions at a center-of-mass energy of 13 TeV and an integrated luminosity of $139 fb^{-1}$.

For the validation of our reimplementation, we have focused on the sector of sparticles with only electroweak interactions. The lightest neutralino ($\tilde{\chi}_1^0$) is taken as the lightest supersymmetric particle (LSP). The stau-left ($\tilde{\tau}_L$) and stau-right ($\tilde{\tau}_R$) are assumed to be mass degenerate without mixing. Therefore the gauge eigenstates ($\tilde{\tau}_L$,$\tilde{\tau}_R$) coincide with the mass eigenstates ($\tilde{\tau}_1$,$\tilde{\tau}_2$). Furthermore, in order to suppress

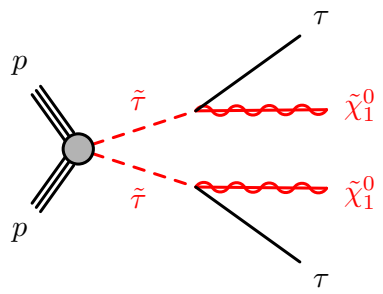

Fig. 1. The Feynman diagram for the process $pp \to \tilde{\tau}\tilde{\tau} \to \tilde{\chi}_1^0\tilde{\chi}_1^0\tau\tau$.

other decay modes of stau, the masses of all charginos and neutralinos are set to 2.5 TeV except for the $\tilde{\chi}_1^0$. Hence, the single kinematically allowed decay mode of stau is

$$\tilde{\tau} \to \tilde{\chi}_1^0\tau \tag{1}$$

2. Description of the analysis

This analysis targets a final state containing two hadronic tau leptons with a certain amount of missing transverse energy. The kinematics of di-$\tau + E_T^{miss}$ system is used to reduce the contributions from Standard Model backgrounds. First, all the objects are reconstructed and defined. Then a sequence of event selections for the signal final state is applied.

2.1. *Object definitions*

Jets are reconstructed by means of the anti-k_t algorithm[7] with a radius parameter set to $R = 0.4$. This analysis focuses on jets whose transverse momentum p_T^j and pseudorapidity η^j fullfill

$$p_T^j > 20 \text{ GeV} \quad \text{and} \quad |\eta^j| < 2.8. \tag{2}$$

Moreover, the selected jets are tagged as originating from the fragmentation of a b-quark with

$$p_T^b > 20 \text{ GeV} \quad \text{and} \quad |\eta^b| < 2.5. \tag{3}$$

A working point with the average b-tagging efficiency of 77% is used. This working point corresponds to a c-jet and light-jet rejection of 4.9 and 110, respectively.

Electron candidates are required to have a transverse momentum p_T^e and pseudorapidity η^e obeying

$$p_T^e > 17 \text{ GeV} \quad \text{and} \quad |\eta^e| < 2.47. \tag{4}$$

Furthermore, all electron candidates are required to have both track and calorimeter isolations. The condition of the track isolation is

$$\sum p_{T,\text{tracks}}/p_T^e < 0.15 \quad \text{with} \quad \Delta R = min(10 \text{ GeV}/p_T^e, 0.2), \tag{5}$$

the condition of the calorimeter isolation is

$$\sum E_{T,\text{calorimeter}}/p_T^e < 0.2 \quad \text{with} \quad \Delta R = 0.2, \tag{6}$$

and for high transverse momentum electron,

$$\sum E_{T,\text{tracks}} < max(0.015 \times p_T^e, 3.5 \text{ GeV}) \quad \text{with} \quad \Delta R = 0.2 \quad \text{if} \quad p_T^e > 200 \text{ GeV}. \tag{7}$$

Muon candidate definition is similar, although with slightly looser thresholds,

$$p_T^\mu > 14 \text{ GeV} \quad \text{and} \quad |\eta^\mu| < 2.7, \tag{8}$$

The condition of the track isolation is

$$\sum p_{T,\text{tracks}}/p_T^\mu < 0.15 \quad \text{with} \quad \Delta R = min(10 \text{ GeV}/p_T^\mu, 0.3), \tag{9}$$

and the condition of the calorimeter isolation is

$$\sum E_{T,\text{tracks}}/p_T^\mu < 0.3 \quad \text{with} \quad \Delta R = 0.2. \tag{10}$$

In the ATLAS experiment, hadronically decaying tau lepton (τ_{had}) candidates are reconstructed with one or three associated charged pion tracks (prongs). For 1-prong (3-prong) τ lepton candidates, the signal efficiencies are 75% and 60% for the *medium* working points. In MADANALYSIS 5 recasting, tau efficiency is set to 100% with misidentification probability of 0% at the DELPHES[15] simulation, and medium and tight tau tagging efficiencies are handled with reweighting factor taken from the official ATLAS cutflow table. Details are described in Sec. 2.2. The baseline tau lepton candidates are required to have

$$p_T^\tau > 50(40) \text{ GeV} \quad \text{and} \quad |\eta^\tau| < 2.5 \tag{11}$$

for the leading (subleading) ones and the transition region between the barrel and endcap calorimeters ($1.37 < |\eta^\tau| < 1.52$) is excluded.

Finally, some overlap removal conditions are in order which are consistent with the analysis code provided in HEPData.[6] Tau lepton is removed if $\Delta R(\tau, e/\mu) < 0.2$. Electron is removed if $\Delta R(e, \mu) < 0.01$. Jet is removed if $\Delta R(j, e/\mu) < 0.2$, and then electron or muon is removed if $\Delta R(e/\mu, j) < 0.4$, and jet is removed if $\Delta R(j, \tau) < 0.4$.

2.2. *Event selection*

On top of object definitions, events with exactly two baseline tau leptons are selected. All events are required to pass either an *asymmetric di-*τ trigger for the low stau mass region (SR-lowMass) or a combined *di-*$\tau + E_T^{miss}$ ($E_T^{miss} > 150$ GeV) trigger for the high stau mass region (SR-highMass) (**Trigger and offline cuts**).

The trigger efficiency about 80% is applied in our recasting with the following offline p_T thresholds for the leading (subleading) tau lepton candidates in Table 1. Assuming the tau leptons fired trigger path are selected in offline event selection, trigger level τ_{had} identification efficiency (~ 0.9) for the offline tau lepton identified with medium identification is applied per selected tau lepton.[17]

Table 1. Offline p_T thresholds for the leading (subleading) tau lepton candidates of *asymmetric di-*τ and *di-*$\tau + E_T^{miss}$ triggers with efficiencies about 80%.

Year	*asymmetric di-*τ	*di-*$\tau + E_T^{miss}$
2015-2017	95 (60) GeV	50 (40) GeV
2018	95 (75) GeV	75 (40) GeV

Then events with exactly two *medium* tau lepton candidates with opposite-sign electric charge (OS) are selected. To treat the efficiency of selecting two offline medium tagged taus on top of *di-tau(+*E_T^{miss}*)* trigger, reweighting factor of 0.7 is applied. It is the ratio of cut efficiencies between ATLAS and recasting result without including medium tau identification at **2 medium** τ **(OS) and 3rd medium** τ **veto** step. Then, b-jet veto is applied to reject events from top quark associated processes. Also, the events with additional light lepton (muon or electron) are rejected. The reconstructed invariant mass of the two leading tau lepton candidates, $m(\tau_1, \tau_2)$, larger than 120 GeV is required for removing tau lepton pair from low-mass resonances, Z boson, and Higgs boson events (Z/H veto).

In SR-lowMass region, values of $75 < E_T^{miss} < 150$ GeV are required for SR-lowMass to increase signal sensitivity. Also, two selected tau leptons are required to be tight tagged. The selection efficiency of two taus passing the *tight* working point on top of two medium tagged tau leptons is taken from official ATLAS cutflow table as a ratio of weighted number of event before and after applying cut ($p_{tight} \simeq 0.70$). On the other hand, in SR-highMass region, the tight tagging efficiency is applied in the same manner as SR-lowMass region, but allowing at least one of two tau leptons passing the tight selection ($p_{tight} + 2\sqrt{p_{tight}}(1 - \sqrt{p_{tight}}) \simeq 0.91$).

The *stransverse mass* m_{T2} variable is defined as[a]

$$m_{T2} = min_{\mathbf{q}_T} \left[max(m_{T,\tau_1}(\mathbf{p}_{T,\tau_1}, \mathbf{q}_T), m_{T,\tau_2}(\mathbf{p}_{T,\tau_2}, \mathbf{p}_T^{miss} - \mathbf{q}_T)) \right], \quad (12)$$

where $\mathbf{p}_{T,\tau_1}$ and $\mathbf{p}_{T,\tau_2}$ are the transverse momenta of the two tau lepton candidates, and the transverse momentum vector of one of the invisible particle, $\mathbf{q}_T$, is choosen to minimize the larger of the two transverse mass m_{T,τ_1} and m_{T,τ_2}. The transverse mass m_T is defined by

$$m_T(\mathbf{p}_T, \mathbf{q}_T) = \sqrt{2(p_T q_T - \mathbf{p}_T \cdot \mathbf{q}_T)}. \quad (13)$$

[a]Notice m_{T2} calculation is done with MADANALYSIS 5 function ($PHYSICS \rightarrow Transverse \rightarrow MT2(vec1, vec2, E_T^{miss}, m_{invisible})$)

A lower bound on the m_{T2} will be imposed to reduce contributions from $t\bar{t}$ and WW events. Finally, the two tau lepton candidates are required to satisfy $\Delta R(\tau_1, \tau_2) < 3.2$, $|\Delta\phi(\tau_1, \tau_2)| > 0.8$ and $m_{T2} > 70$ GeV to further suppress contributions from SM backgrounds.

3. Validation

3.1. *Event generation*

In order to validate our analysis, we rely on the MSSM UFO model file[8] from Feynrules model database.[9] Two benchmark points with masses $m(\tilde{\tau}, \tilde{\chi}_1^0) = (120, 1)$ GeV and $(280, 1)$ GeV are used in this note to illustrate the validation of our reimplementation. We make use of MADGRAPH5 aMC@NLO version 2.6.7[10] for hard-scattering event generation in which leading-order matrix elements are convoluted with the NNPDF23LO[11] parton distribution function (PDF) set. The signal includes the emission of up to two additional partons. We apply the MLM scheme[12,13] of the ME-PS matching with $xqcut = m_{\tilde{\tau}}/4$. Mixing matrix for $\tilde{\tau}$ is set to diagonal to generate separated right- and left-handed $\tilde{\tau}$ samples.

The PYTHIA8 version 8.244[14] with $A14$ tune has been used for the simulation of the parton showering and hadronization. The simulation of the detector response has been performed by using DELPHES-3.4.2,[15] that relies on FASTJET[16] for object reconstruction. The modified delphes card has been used with an appropriate tuned detector card. For example, the loosened isolation criteria are applied to cover all offline object definitions. And the radius parameter of jet and minimum transverse momentum are lowered to 0.4 and 15 GeV with updating b and tau tagging efficiencies. Also, UniqueObjectFinder is disabled for overlap removal which is done in MADANALYSIS5. Finally, we have used the MADANALYSIS5 reimplementation to calculate the signal selection efficiencies.

3.2. *Comparison with the official results*

In Table 2 and 3, we compare the results obtained with our implementation to the official weighted event numbers in the auxiliary tables provided by the ATLAS collaboration for the benchmark points with masses $m(\tilde{\tau}, \tilde{\chi}_1^0) = (120, 1)$ and $(280, 1)$ GeV, respectively. For each cut, we have calculated the related efficiency defined as

$$\epsilon_i = \frac{n_i}{n_{i-1}} \tag{14}$$

where n_i and n_{i-1} mean the event number after and before the considered cut, respectively. On the other hand, we have also calculated the differences between $\epsilon_i(MA5)$ and $\epsilon_i(ATLAS)$ with the definition as

$$diff. = \frac{\epsilon_i(MA5) - \epsilon_i(ATLAS)}{\epsilon_i(ATLAS)} \tag{15}$$

Table 2. Validation checks of the cut flows for $\tilde{\tau}\tilde{\tau}$ production with $m(\tilde{\tau}, \tilde{\chi}_1^0) = (120, 1)$ GeV.

$\tilde{\tau}\tilde{\tau}$ **production with** $m(\tilde{\tau}, \tilde{\chi}_1^0) = (120, 1)$ **GeV**					
	ATLAS($N_{weighted}$)	ϵ_i(%)	MA5($N_{weighted}$)	ϵ_i(%)	diff.(%)
Baseline cut	1686.80	-	1686.80	-	-
SR-low Mass					
Trigger and offline cuts	390.46	23.15	410.01	24.31	5.01
2 medium τ (OS) and 3rd medium τ veto	256.01	65.57	269.37	65.70	0.20
b-jet veto	250.59	97.88	263.66	97.88	-0.00
Light lepton veto	250.12	99.81	263.66	100	0.19
Z/H-veto	248.93	99.52	262.14	99.42	-0.10
$75 < E_T^{miss} < 150$ GeV	85.70	34.43	89.90	34.30	-0.38
2 tight τ	60.19	70.23	62.93	70.00	-0.33
$\lvert\Delta\phi(\tau,\tau)\rvert > 0.8$	60.14	99.92	62.75	99.72	-0.20
$\lvert\Delta R(\tau,\tau)\rvert < 3.2$	54.73	91.00	57.10	90.99	-0.01
$m_{T2} > 70$ GeV	9.78	17.87	14.65	25.66	43.58
All	-	0.58	-	0.87	49.80
SR-high Mass					
Trigger and offline cuts	101.23	6.00	96.35	5.71	-4.82
2 medium τ (OS) and 3rd medium τ veto	67.04	66.23	63.23	65.62	-0.91
b-jet veto	63.98	95.44	60.37	95.47	0.04
Light lepton veto	63.87	99.83	60.36	99.99	0.16
Z/H-veto	58.33	91.33	55.70	92.28	1.04
≥ 1 tight τ	57.29	98.22	50.69	91.00	-7.35
$\lvert\Delta\phi(\tau,\tau)\rvert > 0.8$	56.71	98.99	49.99	98.63	-0.36
$\lvert\Delta R(\tau,\tau)\rvert < 3.2$	51.74	91.24	45.41	90.84	-0.43
$m_{T2} > 70$ GeV	7.18	13.88	8.24	18.14	30.75
All	-	0.43	-	0.49	14.76

We observe that the disagreement on a cut-by-cut basis, is 49.8% and 14.76% with all cuts for SR-lowMass and SR-highMass in Table 2 of $m(\tilde{\tau}, \tilde{\chi}_1^0) = (120, 1)$ GeV. The major parts of the disagreement come from m_{T2} cut steps. By lack of more public experimental information, we have not been able to validate the step more precisely. In Fig. 2, we realize the m_{T2} distributions from ATLAS analysis are softer than our results with large uncertainties. This causes the $m_{T2} > 70$ GeV cut looser in our reimplementation than the original ATLAS results which is taken from HEPData.[6]

Similarly, the disagreement on a cut-by-cut basis is -7.24% and -6.84% with all cuts for SR-lowMass and SR-highMass in Table 3 of $m(\tilde{\tau}, \tilde{\chi}_1^0) = (280, 1)$ GeV. Again, the major parts of the disagreement come from m_{T2} cut step as well as **Trigger and offline cuts** in SR-higsMass region. The m_{T2} distributions are shown in Fig. 3 for the comparison of our results with ATLAS analysis.

4. Conclusions

We have implemented the ATLAS-SUSY-2018-04 search in the MADANALYSIS 5 framework. Our analysis has been validated in the context of a supersymmetry-inspired simplified benchmark model in which the Standard Model is extended by

Table 3. Validation checks of the cut flows for $\tilde{\tau}\tilde{\tau}$ production with $m(\tilde{\tau}, \tilde{\chi}_1^0) = (280, 1)$ GeV.

$\tilde{\tau}\tilde{\tau}$ **production with** $m(\tilde{\tau}, \tilde{\chi}_1^0) = (280, 1)$ **GeV**					
	ATLAS($N_{weighted}$)	ϵ_i(%)	MA5($N_{weighted}$)	ϵ_i(%)	diff.(%)
Baseline cut	184.36	-	184.36	-	-
SR-low Mass					
Trigger and offline cuts	73.74	40.00	69.97	37.95	-5.12
2 medium τ (OS) and 3rd medium τ veto	47.86	64.90	46.23	66.08	1.81
b-jet veto	46.63	97.43	44.94	97.20	-0.24
Light lepton veto	46.49	99.70	44.94	99.99	0.30
Z/H-veto	44.84	96.45	43.83	97.54	1.13
$75 < E_T^{miss} < 150$ GeV	17.48	38.98	16.26	37.10	-4.83
2 tight τ	12.04	68.88	11.38	70.00	1.63
$\lvert\Delta\phi(\tau,\tau)\rvert > 0.8$	12.04	100	11.33	99.55	-0.45
$\lvert\Delta R(\tau,\tau)\rvert < 3.2$	11.08	92.03	10.35	91.32	-0.77
$m_{T2} > 70$ GeV	6.08	54.87	5.64	54.50	-0.68
All	-	3.30	-	3.06	-7.24
SR-high Mass					
Trigger and offline cuts	47.64	25.84	42.10	22.83	-11.64
2 medium τ (OS) and 3rd medium τ veto	30.72	64.48	27.80	66.03	2.40
b-jet veto	29.34	95.51	26.83	96.52	1.06
Light lepton veto	29.27	99.76	26.83	99.99	0.23
Z/H-veto	24.88	85.00	24.01	89.50	5.30
≥ 1 tight τ	24.21	97.31	21.85	91.00	-6.48
$\lvert\Delta\phi(\tau,\tau)\rvert > 0.8$	23.29	96.20	21.19	96.96	0.79
$\lvert\Delta R(\tau,\tau)\rvert < 3.2$	21.95	94.25	19.68	92.91	-1.42
$m_{T2} > 70$ GeV	14.35	65.38	13.37	67.91	3.88
All	-	7.78	-	7.25	-6.84

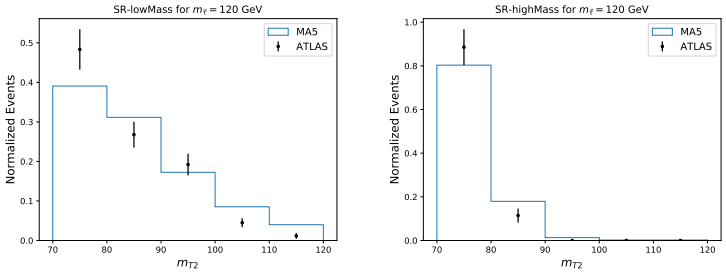

Fig. 2. The m_{T2} distributions for $m(\tilde{\tau}, \tilde{\chi}_1^0) = (120, 1)$ GeV.

a neutralino and a stau decaying into a tau lepton and a neutralino, employing two different benchmark points in the parameter space. By comparing our predictions for the cutflow with the official one provided by ATLAS in Ref.,[5] we have found an agreement for each step in Table 2 and 3 except for the ones from **Trigger and offline cuts** and m_{T2} cut. Due to the lack of more information, we have not been able to validate these steps more precisely.

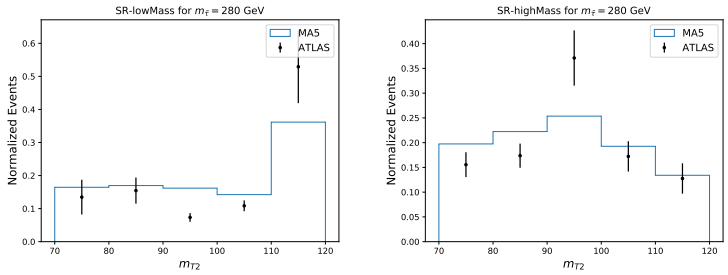

Fig. 3. The m_{T2} distributions for $m(\tilde{\tau}, \tilde{\chi}_1^0) = (280, 1)$ GeV.

Acknowledgments

Dedications and funding information may be included here.

References

1. E. Conte and B. Fuks, Int. J. Mod. Phys. A **33** (2018) no.28, 1830027 [arXiv:1808.00480 [hep-ph]].
2. B. Dumont *et al.*, Eur. Phys. J. C **75** (2015) no.2, 56 [arXiv:1407.3278 [hep-ph]].
3. E. Conte, B. Dumont, B. Fuks and C. Wymant, Eur. Phys. J. C **74** (2014) no.10, 3103 [arXiv:1405.3982 [hep-ph]].
4. E. Conte, B. Fuks and G. Serret, Comput. Phys. Commun. **184** (2013) 222 [arXiv:1206.1599 [hep-ph]].
5. G. Aad *et al.* [ATLAS Collaboration], Phys. Rev. D **101**, no. 3, 032009 (2020) doi:10.1103/PhysRevD.101.032009 [arXiv:1911.06660 [hep-ex]].
6. G. Aad *et al.* [ATLAS], doi:10.17182/hepdata.92006
7. M. Cacciari, G. P. Salam and G. Soyez, JHEP **0804**, 063 (2008) doi:10.1088/1126-6708/2008/04/063 [arXiv:0802.1189 [hep-ph]].
8. C. Duhr and B. Fuks, Comput. Phys. Commun. **182**, 2404 (2011) doi:10.1016/j.cpc.2011.06.009 [arXiv:1102.4191 [hep-ph]].
9. A. Alloul, N. D. Christensen, C. Degrande, C. Duhr and B. Fuks, Comput. Phys. Commun. **185**, 2250 (2014) doi:10.1016/j.cpc.2014.04.012 [arXiv:1310.1921 [hep-ph]].
10. J. Alwall *et al.*, JHEP **1407**, 079 (2014) doi:10.1007/JHEP07(2014)079 [arXiv:1405.0301 [hep-ph]].
11. A. D. Martin, W. J. Stirling, R. S. Thorne and G. Watt, Eur. Phys. J. C **63**, 189 (2009) doi:10.1140/epjc/s10052-009-1072-5 [arXiv:0901.0002 [hep-ph]].
12. M. L. Mangano, M. Moretti, F. Piccinini and M. Treccani, JHEP **0701**, 013 (2007) doi:10.1088/1126-6708/2007/01/013 [hep-ph/0611129].
13. J. Alwall, S. de Visscher and F. Maltoni, JHEP **0902**, 017 (2009) doi:10.1088/1126-6708/2009/02/017 [arXiv:0810.5350 [hep-ph]].
14. T. Sjostrand, S. Mrenna and P. Z. Skands, Comput. Phys. Commun. **178**, 852 (2008) doi:10.1016/j.cpc.2008.01.036 [arXiv:0710.3820 [hep-ph]].
15. J. de Favereau *et al.* [DELPHES 3 Collaboration], JHEP **1402**, 057 (2014) doi:10.1007/JHEP02(2014)057 [arXiv:1307.6346 [hep-ex]].
16. M. Cacciari, G. P. Salam and G. Soyez, Eur. Phys. J. C **72**, 1896 (2012) doi:10.1140/epjc/s10052-012-1896-2 [arXiv:1111.6097 [hep-ph]].

17. ATLAS Collaboration, ATLAS-CONF-2017-029.